

**This is the preprint of the contribution published as:**

**Rago, L., Popp, D., Heiker, J.T., Harnisch, F.** (2021):  
Electroactive microorganisms in mouse feces  
*Electrochim. Acta* **365** , art. 137326

**The publisher's version is available at:**

<http://dx.doi.org/10.1016/j.electacta.2020.137326>

# Electroactive microorganisms in mouse feces

Laura Rago<sup>[a]</sup>, Denny Popp<sup>[a]</sup>, John T. Heiker<sup>[b]</sup>, Falk Harnisch<sup>\*[a]</sup>

---

[a] Department of Environmental Microbiology  
Helmholtz Centre for Environmental Research GmbH – UFZ  
Permoserstrasse 15, 04318 Leipzig, Germany  
\*Corresponding author Prof. Dr. Falk Harnisch  
falk.harnisch@ufz.de

[b] Helmholtz Institute for Metabolic, Obesity and Vascular Research (HI-MAG) of the Helmholtz Zentrum München at the University of Leipzig and University Hospital Leipzig  
Philipp-Rosenthal-Str. 27, 04103 Leipzig, Germany

Supporting information for this article is given via a link at the end of the document

**Abstract:** The gut microbiome is not only an indicator of different pathologies, but it also influences metabolism and overall health of the host. Recently, microorganisms inherent to the gut microbiome, such as *Listeria monocytogenes*, *Enterococcus faecalis* and *Clostridium cochlearium*, were demonstrated to be electroactive, i.e. to perform extracellular electron transfer (EET). To further explore the presence of electroactive microorganisms in the gut microbiome electrochemical enrichment starting from mouse feces was performed. Open circuit, abiotic and autoclaved inoculum controls were run in parallel. A maximum current density of  $122\pm 23 \mu\text{A cm}^{-2}$  at low coulombic efficiency (~1%) was achieved. The presence of biofilms at the anode and microbial electrochemical activity with a formal potential of EET of  $0.23\pm 0.01 \text{ V vs. Ag/AgCl sat. KCl}$  was demonstrated using fluorescence microscopy and cyclic voltammetry. The 16S rRNA gene sequencing and PCR-free Nanopore sequencing showed the enrichment and dominance of *Shigella flexneri*.

**Keywords:** Extracellular Electron Transfer (EET) • gut microbiome • electroactive microorganisms • next generation sequencing (NGS) • whole genome sequencing (WGS)

## 1. Introduction

The rising interest on the mammalian and especially the human gut microbiome is triggered by the close relationship between its composition and activity and the health of the host. This makes the gut microbiome not only an indicator of different pathologies, but also a controller of wellness and disease [1]. In biological and biomedical research, animal models, especially mice and rats, serve as models for studying the effects of the gut microbiome on the occurrence and development of diseases [2,3].

Electroactive microorganisms perform extracellular electron transfer (EET) that allows linking their metabolism with the oxidation or the reduction of the respective electron donors or acceptors that cannot enter the cell [4]. It was shown that electroactive microorganisms can create complex food webs and occupy a high diversity of ecological niches [4]. Recently, it was revealed that the gut is also a possible habitat for electroactive microorganisms. A mediated EET mechanism based on flavin was demonstrated for the food-borne pathogen *Listeria monocytogenes* [5,6]. Further, it was demonstrated that the commensal members of the mouse gut microbiome, being selected from the Mouse Intestinal Bacterial Collection [7], *Clostridium cochlearium*, *Lactobacillus reuteri* and *Staphylococcus xylosus*, can be electroactive [8] as also demonstrated for the opportunistic human pathogen *Enterococcus faecalis* [9]. Recently, Naradasu et al. [10] have shown EET of two oral biofilm pathogens: *Aggregatibacter actinomycetemcomitans* and *Porphyromonas gingivalis*.

However, only few studies aimed to explore the further presence of electroactive microorganisms and the role of EET of a natural gut microbiome being a highly diverse microbial mixed culture. Wang et al. [11], cultured the cecal microbiome of C57BL/6 mice *in-vitro* with the addition of flavin, showing the flavin-based EET using cyclic voltammetry (CV). Moreover, the CV was performed in intact guts of mice, showing *in vivo* the capability of EET of the gut microbiome. Naradasu et al. [12] electrochemically enriched the microorganisms from a not characterized human fecal sample of one donor, for around two weeks. The EET capability of the microorganisms enriched on the anode were then tested on  $\delta$ -MnO<sub>2</sub> microbial culture plates, showing the putative EET capability of two isolated strains *Enterococcus avium* and *Klebsiella pneumoniae*. Another study [13], aimed to explore the current production in a single-chamber microbial electrolysis cell exploring the EET capability of fecal inoculum collected from C57BL/6J and C57BL/6NHsd and hypothesizing the interaction between the gut microbiota and the recruitment of cells of the immune system to the gut.

These few studies clearly demonstrate that several microorganisms colonizing the mammalian digestive tract are able to be electroactive meaning to perform EET with physiological relevance [14]. Thus, one may hypothesize that the use of an external solid terminal electron acceptor or donor (e.g. an electrode, but also a solid conductive material having the function of an electron bridge), can be used to influence the gut microbial community composition, metabolism and hence function. This may allow to speculate that electrochemical stimulation of the gut microbiome may be a future tool with huge potential impact, for both, microbiology and medicine.

Here, we systematically investigated the gut as habitat of electroactive microorganisms, inoculating glucose-fed two-chamber bioelectrochemical systems (BES) with mixed feces from

common laboratory mouse strain for around 1 month. The formed anodic biofilm was studied by electrochemical-based techniques (chronoamperometry and cyclic voltammetry) and the use of next generation sequencing (NGS) and whole genome sequencing (WGS).

## 2. Material and methods

All chemicals were of at least analytical grade and were supplied from Carl Roth GmbH (Karlsruhe, Germany) and Merck KGaA (Darmstadt, Germany). De-ionized water (Millipore, Darmstadt, Germany) was used to prepare the microbial growth media, substrate and buffer solutions. All potentials provided in this article refer to the Ag/AgCl sat. KCl reference electrode (+197 mV vs. standard hydrogen electrode (SHE)). All values are provided as average  $\pm$  standard deviation, based on independent triplicates (n=3).

### 2.1. Setup of bioelectrochemical systems and medium composition

The reactors consisted of two-chamber bioelectrochemical systems (BES) made of 100 mL glass bottles (Duran<sup>®</sup>, München, Germany) with 90 mL working volume. The working electrode (WE) and counter electrode were graphite rods (CP Handels GmbH, Wachtberg, Germany) with a geometric surface area of 7.26 cm<sup>2</sup>. The WE and reference electrode (RE, SE 11 Ag/AgCl sat. KCl reference electrode (+197 mV vs. SHE, Xylem Analytics Germany Sales GmbH & Co/ Meinsberg Sensortechnik GmbH, Germany)) were assembled in a butyl rubber stopper. The counter electrode chamber of 15 mL volume was partially immersed in the WE chamber via a butyl rubber stopper. Thus, the counter electrode was physically separated but ionically connected to the WE chamber via a membrane (fumasep<sup>®</sup> FKE, Fumatech, Bietigheim-Bissingen, Germany).

Before and after each experiment the WE surface were cleaned with sandpaper (WetorDry P1200, 3M, Minnesota, USA). The medium used in the WE chamber was obtained modifying the Firmicutes Minimal Medium (modified YFCA) [8,15,16] adding glucose 0.5 % (w/v) and removing the peptone, the yeast extract, the haematin and resazurin as alternative electron donors and acceptors thus containing: 0.45 g L<sup>-1</sup> K<sub>2</sub>HPO<sub>4</sub>; 0.45 g L<sup>-1</sup> KH<sub>2</sub>PO<sub>4</sub>; 0.90 g L<sup>-1</sup> NaCl; 0.90 g L<sup>-1</sup> (NH<sub>4</sub>)<sub>2</sub>SO<sub>4</sub>; 0.09 g L<sup>-1</sup> MgSO<sub>4</sub> × 7H<sub>2</sub>O; 4 g L<sup>-1</sup> NaHCO<sub>3</sub>; 0.12 g L<sup>-1</sup> CaCl<sub>2</sub> × 2H<sub>2</sub>O; 1 g L<sup>-1</sup> L-Cysteine HCl; 1 mL L<sup>-1</sup> Vitamine solution for Firmicutes (0.01 g L<sup>-1</sup> Biotin; 0.01 g L<sup>-1</sup> B 12; 0.03 g L<sup>-1</sup> p-aminobenzoic acid; 0.05 g L<sup>-1</sup> folic acid; 0.15 g L<sup>-1</sup> Pyridox HCl ) and glucose 0.5 % (w/v). The counter electrode chamber was filled with 10 mL of a phosphate buffer solution (70 g L<sup>-1</sup> Na<sub>2</sub>HPO<sub>4</sub> and 12 g L<sup>-1</sup> KH<sub>2</sub>PO<sub>4</sub>).

The PBS used to dilute the mouse feces, consisted of 8 g L<sup>-1</sup> NaCl, KCl 0.2 g L<sup>-1</sup>, 1.44 g L<sup>-1</sup> Na<sub>2</sub>HPO<sub>4</sub> and 0.24 g L<sup>-1</sup> KH<sub>2</sub>PO<sub>4</sub>.

### 2.2. Experimental design and inoculum

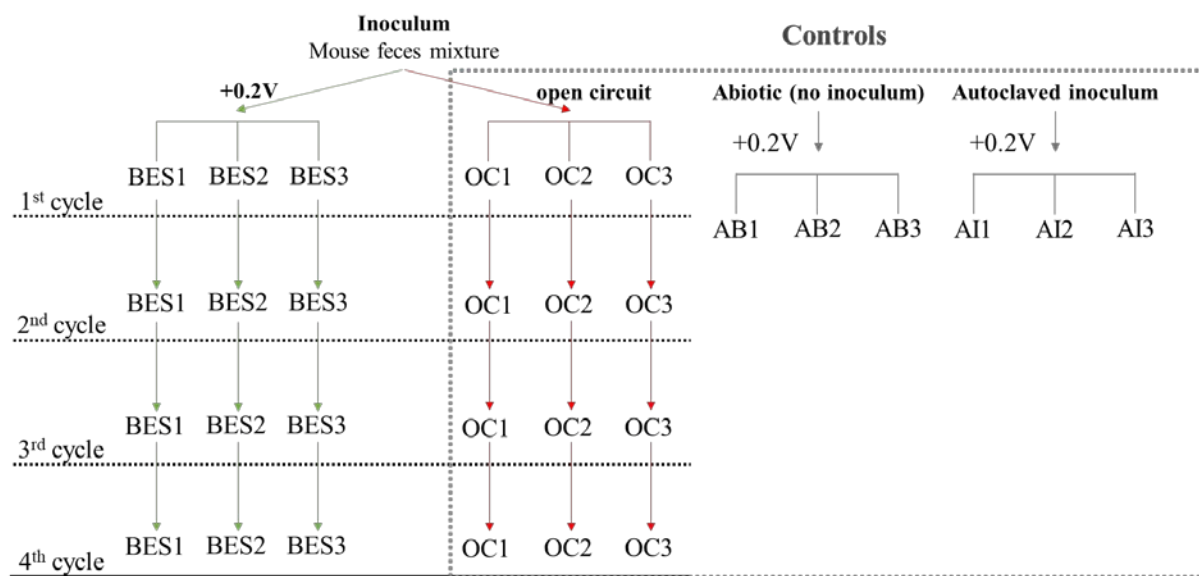
The experimental design (Scheme 1), consisted of each three replicate BES and three controls including open circuit controls (OC), i.e. BES without applying a potential, the abiotic controls, i.e. reactors without inoculum, and the BES being inoculated with autoclaved inoculum.

The BES and the OC reactors were inoculated using a mouse feces mixture consisting of a mixture of 100 pieces of male C57BL/6NTac fresh mouse feces in 20 mL of sterile PBS (stored for up to 24 h at 4°C). All BES were started immediately and operated using chronoamperometry

(CA) at 0.2 V in parallel for four batch cycles (~one week each). Thus, no pre-enrichment from the feces took place.

After each batch cycle, 90% of the medium was replaced for fresh anoxic medium. The WE chamber was closed gas tight and gently flushed with sterile N<sub>2</sub> for further 10 minutes, to keep the anoxic environment. All experiments were carried out under potentiostatic control using a multi-channel potentiostat/galvanostat (MPG-2/VSP, BioLogic Science Instruments, Claix, France) at 30 °C (Unihood Uniequip, Planegg, Germany) and stirred at 120 rpm (2mag, München, Germany). For cyclic voltammetry (CV) three cycles were recorded at the beginning of the batch cycle, at the maximum of the current production (turnover conditions). All the CVs were performed in a scan range from -0.1 to +0.65 V starting at 0.2V and with a scan rate of 1 mV s<sup>-1</sup>. The scan range was limited to exclude high-potential side effects, but still including the potential applied to the WE (+0.2V). The formal potential of the EET ( $E^f$ ) was identified using 1<sup>st</sup> derivatives of turnover CVs of the 3<sup>rd</sup> CV cycle showing steady state.

The abiotic reactors were identical to the BES, but without the addition of the inoculum. The autoclaved inoculum reactors were setup using as inoculum the identical mouse feces mixture being autoclaved (121°C, 20 min - HMC Europe GmbH, Tüßling, Germany) 5 times. The abiotic and the autoclaved inoculum reactors were run using CA at +0.2 V for 6 days. Noteworthy, when using inoculum of the same source, the identical base medium, but instead of glucose only short chain fatty acids (0.018 g L<sup>-1</sup> of acetate, 0.042 g L<sup>-1</sup> of propionate, 0.05 g L<sup>-1</sup> of butyrate) as carbon source, no current production was detected.



**Scheme 1.** Schematic summary of the experimental design (details see text).

### 2.3. Chemical analysis

The BES were sampled for HPLC analysis at the end of each batch cycle and high-performance-liquid-chromatography (HPLC) was performed. Therefore, after the centrifugation (13000 × g, 10

min) of the used media the supernatant was filtered (0.2 µm pore size, nylon, Sartorius, Göttingen, Germany) before HPLC analyses (Shimadzu Scientific Instruments, Kyoto, Japan) using a HiPlex H column (300 x 7.7 mm, 8 µm pore size, Agilent Technologies, Santa Clara, USA) with 5 mM H<sub>2</sub>SO<sub>4</sub> as mobile phase (0.5 mL min<sup>-1</sup> and 50 °C) using a refractive index detector (RID-10A). The signal was calibrated for glucose, formate, acetate, propionate, butyrate, pyruvate and succinate in the range of 0.02 g L<sup>-1</sup> to 1 g L<sup>-1</sup> (R<sup>2</sup>=0.99) A Micro GC Gas Analyzer (INFICON, Cologne, Germany) was used [17] for head space gas analysis at the end of the 1<sup>st</sup> and the 4<sup>th</sup> cycle.

For pH measurements a pH meter was used (LaquaTwin B-712, Horiba Scientific, Bensheim, Germany).

## 2.4. Calculations and Statistics

In order to determine the efficiency of microbial current production, the coulombic efficiency (*CE*) was calculated [Eq. 1].

$$\text{Eq. 1: } CE = n_{e^-}(\text{real}) / n_{e^-}(\text{theoret.}) \times 100$$

The molar amount of electrons ( $n_{e^-}(\text{real})$ ) is calculated from the total charge ( $q_{\text{tot}}$ ) recorded during CA divided by the Faraday constant ( $F = 96485.33 \text{ C mol}^{-1}$ ) [Eq. 2].

$$\text{Eq. 2: } n_{e^-}(\text{real}) = q_{\text{tot}} / F$$

The theoretical number of electrons ( $n_{e^-}(\text{theoret.})$ ) is calculated as:

$$\text{Eq. 3: } n_{e^-}(\text{theoret.}) = q_{\text{thGLUC}} - q_{\text{thRES}}$$

Where  $q_{\text{thGLUC}}$  is representing the charge that can be gained from the glucose measured at the beginning of the batch cycle when being completely oxidized to CO<sub>2</sub>, and the  $q_{\text{thRES}}$  is the residual charge of each of the compounds (glucose, formate, acetate, propionate, butyrate, pyruvate and succinate) when being completely oxidized to CO<sub>2</sub> measured at the end of the batch cycle.

**Table 1. Compounds and reactions for complete oxidation to CO<sub>2</sub> and number of electrons  $n_{e^-}(\text{theoret.})$  involved.**

Compounds	Chemical oxidation reaction to CO <sub>2</sub>	$n_{e^-}(\text{theoret.})$
<b>Glucose</b>	$\text{C}_6\text{H}_{12}\text{O}_6 + 6\text{H}_2\text{O} \rightarrow 6\text{CO}_2 + 24\text{H}^+ + 24\text{e}^-$	24
<b>Formate</b>	$\text{HCOO}^- \rightarrow \text{CO}_2 + \text{H}^+ + 2\text{e}^-$	2
<b>Acetate</b>	$\text{CH}_3\text{COO}^- + 2\text{H}_2\text{O} \rightarrow 2\text{CO}_2 + 7\text{H}^+ + 8\text{e}^-$	8
<b>Propionate</b>	$\text{C}_3\text{H}_5\text{O}_2^- + 4\text{H}_2\text{O} \rightarrow 3\text{CO}_2 + 13\text{H}^+ + 14\text{e}^-$	14
<b>Butyrate</b>	$\text{C}_4\text{H}_7\text{O}_2^- + 6\text{H}_2\text{O} \rightarrow 4\text{CO}_2 + 19\text{H}^+ + 20\text{e}^-$	20
<b>Pyruvate</b>	$\text{C}_3\text{H}_3\text{O}_3^- + 3\text{H}_2\text{O} \rightarrow 3\text{CO}_2 + 9\text{H}^+ + 10\text{e}^-$	10
<b>Succinate</b>	$\text{C}_4\text{H}_5\text{O}_4^- + 4\text{H}_2\text{O} \rightarrow 4\text{CO}_2 + 13\text{H}^+ + 14\text{e}^-$	14

The potential shift, as function of pH was calculated using the Nernst equation (Eq. 4):

$$\text{Eq. 4: } E_{fGLUC} = E^\circ_{GLUC} - \frac{RT}{nF} \ln \left( \frac{C_{GLUC}}{p_{\text{CO}_2} \cdot C_{\text{H}^+}^{24}} \right)$$

Here,  $E_{fGLUC}$  is the formal potential of the glucose oxidation;  $E^{\circ}_{GLUC}$  is the standard potential of the chemical oxidation reaction of the glucose to  $CO_2$  in standard conditions;  $R$  is the universal gas constant;  $T$  is the temperature in Kelvin;  $F$  is the Faraday constant;  $n$  is the number of electrons transferred in the cell during the chemical oxidation reaction of the glucose to  $CO_2$  (see Table 1);  $C_{GLUC}$  is the glucose concentration; the  $p_{CO_2}$  is the partial pressure of carbon dioxide (assumed value of 0.1 atm) and  $C_{H^+}$  is the concentration of  $H^+$  at the specific pH at 30°C. In this way, the theoretical potential shift, in line with the experimental data, was determined to be -0.2 V from pH 8.1 ( $E_{fGLUC} = -0.73$  V) to pH 4.8 ( $E_{fGLUC} = -0.53$  V).

## 2.5. Electrochemical in-depth study

At the end of the 1<sup>st</sup> and the 4<sup>th</sup> cycle, each original BES was split in three different components (the WE, the planktonic cells and the supernatant) that were studied individually in fresh BES using CV as follows: A) the WE was moved to a new BES containing 90 mL of fresh medium (pH= 8.1); B) the planktonic cells, i.e. the cell pellet obtained by centrifuging 30 mL of the used medium (6000 × g, 10 min, 4°C), was anaerobically re-suspended in 90 mL of fresh medium and transferred to a new sterile BES; C) the supernatant derived from centrifugation of 30 mL of the used medium was anaerobically mixed with 60 mL of fresh medium and transferred to a new BES (Scheme SI-1).

The CVs were recorded (as described before) at the beginning of the batch cycle. Subsequently to CV analysis the BES built using the WE (A) and the cells (B), were run using CA for a full batch cycle (7 days) at the end of the experiment (4<sup>th</sup> cycle).

## 2.6. DNA extraction

Three different type of samples were obtained during the experiment and DNA was extracted using QIAamp PowerFecal DNA Kit (QIAGEN, Hilden, Germany) according to the manufacturer's instructions. The inoculum sample consisted of 300 µL of the mouse feces mixture used to inoculate the reactors. The pellet samples were obtained from each BES, by centrifuging 30 mL of the used medium (6000 × g, 10 min, 4°C), at the end of each batch cycle. The WE samples were obtained from the electrodes of the BES at the end of the experiment and consisted in 1.5 cm of the WE graphite rods, gently rinsed with Millipore water.

## 2.7. Illumina MiSeq amplicon sequencing and PCR-free Nanopore sequencing

The V3/V4 region of the 16S rRNA gene of the extracted genomic DNA was sequenced using the bacterial primers 341F-785R [18] by LGC Genomics GmbH (Berlin, Germany) following their protocols. Raw sequence data have been submitted to the EMBL ENA database under the accession number PRJNA623009. The amplicon reads were pre-processed by removing the primer sequences using cutadapt version 2.7 [19]. Forward and reverse reads were denoised and merged using the dada2 plugin [20] in QIIME2 version 2019.1 [21]. In detail, maximum expected errors were set to 8 and chimeric sequences were removed in default consensus mode of the dada2 plugin. Resulting ASVs were taxonomically classified using MiDAS taxonomy 2.1 [22] trimmed to the region covered by the 341f and 785r primers. Read counts were normalized to 100%.

Whole genome sequencing (WGS) was performed by PCR-free Nanopore sequencing. Genomic DNA from samples of the WE and cell pellet obtained from BES1 after the 4<sup>th</sup> batch cycle and OC1 after 4<sup>th</sup> cycle was prepared for sequencing using the SQK-LSK 109 Ligation Sequencing Kit in combination with EXP-NBD104 Native Barcoding Expansion Kit according to the manufacturer's instructions with the following modifications. The incubation times for the end-repair were increased to 10 min at room temperature and 10 min at 65°C and of the ligation step to 30 min. DNA library was loaded on a R9.4.1 flow cell plugged into a Minlon MK1B device (Oxford Nanopore Technologies, UK) controlled by MinKnow software release 19.12.2. In total 81 Mb, 507 Mb and 435 Mb were obtained for WE, BES1 and OC1 sample, respectively. Raw sequence data have been submitted to the EMBL ENA database under the accession number PRJNA623009. Sequence data were basecalled and demultiplexed using guppy version 3.4.3 and the provided high accuracy model. Adapter sequences were trimmed using Porechop version 0.2.4 (<https://github.com/rrwick/Porechop>). Composition of microbial community was assessed based on the reads using kaiju version 1.7.3 [23] and the proGenomes database. Reads were corrected and assembled using Canu version 1.9 [24] to reconstruct genomes. Resulting contigs were binned using concoct version 1.1.0 [25]. Contigs of the largest bin of each sample were polished using medaka version 0.11.4 (<https://github.com/nanoporetech/medaka>) and taxonomically characterized using the Microbial Genomes Online Atlas [26] and GTDB-tk hosted on KBase [27]. Completeness and contamination of reconstructed genomes were estimated using checkM version 5.0.2 and the lineage-specific workflow [28]. The metagenome assembled genomes (MAGs) obtained from the different samples were compared using dRep [29].

The MAGs were annotated using RASTtk via The Pathosystems Resource Integration Center [30]. The putative marker genes for electroactivity [31,32], already used in a previous study [8], cytochromes, Pilin, PilA, Ferredoxin, Nanotubes (Ymdb) and Phosphodiesterase were analyzed. Distilled and Refined Annotation of Metabolism tool (<https://github.com/shafferm/DRAM>) was used to get a functional annotation summarized on the pathway level (SI-4 and SI-5 files)

Pure culture studies under different conditions are required for the full electroactive metabolism understanding. Unfortunately, the whole *Shigella/Escherichia* genus belongs to biosafety level (BSL) 2, which represents an impediment to perform further studies in mixed and/or culture in laboratories not authorized by law. Thus, all the samples obtained for this study, were destroyed.

## 2.8. Microscopy

One piece obtained from the WE of each BES at the end of the experiment, was used to visualize the biofilm marked with the nucleic acid staining kit LIVE/DEAD<sup>®</sup> BacLight<sup>™</sup> Bacterial Viability Kit (Life technologies, Carlsbad, California, USA) using an Axio Observer.Z1 fluorescence microscope (Carl Zeiss Microscopy GmbH, Jena, Germany) equipped with an Illuminator HXP 120 V, a plan-apochromat 63x/1.40 Oil Ph3 M27 objective, an AxioCam MR3 camera and Axiovision software version 4.83 SP3 was used .

## 3. Results and discussions

Glucose-fed two-chamber bioelectrochemical systems (BES) being inoculated with mixed feces from the common inbred strain of C57BL/6NTac mice were operated using chronoamperometry

(CA) at 0.2 V (as all potentials in this article provided vs. Ag/AgCl sat. KCl). Cultivation was performed without pre-enrichment and for four batch cycles with one week per cycle (see Figure 1).

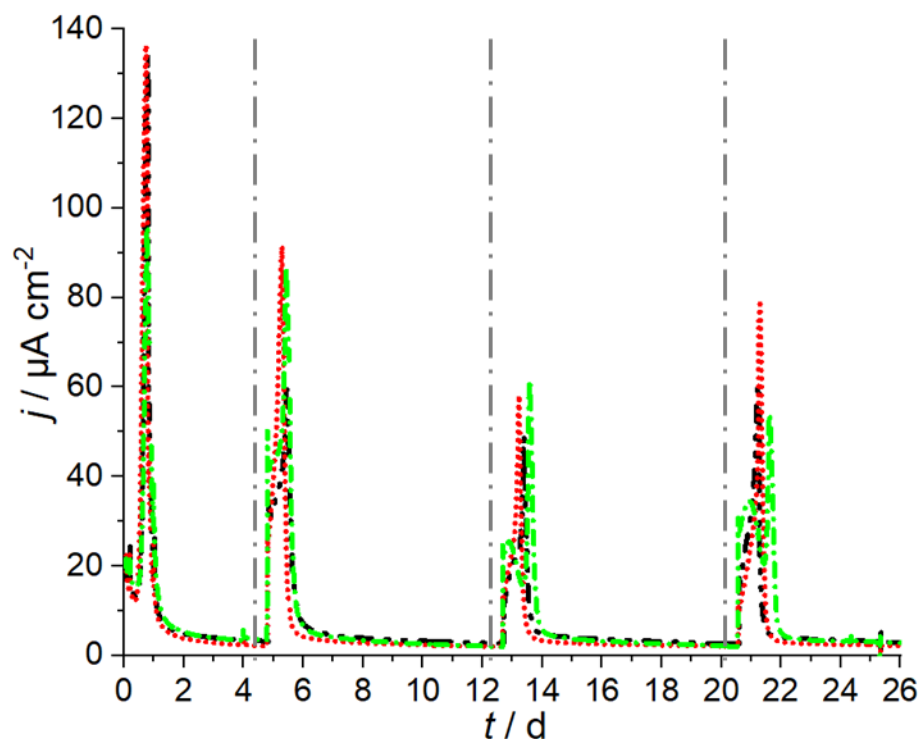


**Figure 1:** Current density ( $\mu\text{A cm}^{-2}$ ) of glucose fed bioelectrochemical systems (BES) inoculated with mouse feces polarized at +0.2 V vs. Ag/ AgCl sat. KCl (30 °C and 120 rpm) for four batch cycles (the gray vertical dotted lines indicate the starting of each cycle). The color of the traces refers to the three independent replicates: red for BES1, black for BES2 and green for BES3.

Figure 1 shows a maximum current density ( $j_{\text{max}}$ ) of  $122\pm 23 \mu\text{A cm}^{-2}$  was achieved during the first batch cycle, which decreased after the first medium change (90% fresh medium + 10% old medium) to  $79.31\pm 17.30 \mu\text{A cm}^{-2}$  (Table 1). The current production started after only 19 hours of CA, which indicates the presence of electroactive microorganisms in the inoculum and it is coherent with previous studies on pure and mixed cultures [8,13].

The average coulombic efficiency ( $CE$ , Table 1) of the four cycles was  $0.93\pm 0.17\%$  ( $n=3$ ). The reason of such a low  $CE$  is unknown, but in-line with the scarcely reported  $CE$  of electroactive microorganisms inherent to the gut microbiome [8]. Partially it can be attributed to the sulfate acting as terminal electron acceptor ( $\sim 500$  C per BES being  $<10\%$  of the  $CE$ ). Gas chromatography (GC) at the end of the 1<sup>st</sup> and the 4<sup>th</sup> cycles confirmed that methanogenesis does not play role (methane under detection limit,  $n=12$ ). Further, metagenomic analysis (PCR-free Nanopore sequencing), confirmed the metabolic diversity and the absence of methanogens in the microbial community (see below). In addition, the presence of oxygen in the reactor headspaces was excluded by GC analysis at the end of the 1<sup>st</sup> and the 4<sup>th</sup> bioelectrochemical cycles.

In contrast to other studies, controls including open circuit, abiotic and autoclaved inoculum reactors were operated in parallel (details see Table 2 and Figure SI-5). Thereby, the abiotic and the autoclaved inoculum reactors showed significantly lower electrochemical performance than the BES being inoculated with feces (Figure SI-5).

**Table 2:** The average of the total charge ( $q$ ), the maximum current density ( $j_{max}$ ) and the coulombic efficiency ( $CE$ ) are reported for the bioelectrochemical systems (BES) for each batch cycle, for the abiotic and the autoclaved inoculum reactors. The formal potential ( $E^f$ ) was calculated from the 3<sup>rd</sup> scan of turnover cyclic voltammetry using  $1 \text{ mV s}^{-1}$  after the 1<sup>st</sup> and the 4<sup>th</sup> batch cycle. Further, the averaged values ( $n=3$ ) were reported for the split BES reactors built using the cells and the working electrodes (WEs) of the BES after the batch cycle. All values are provided as average  $\pm$  standard deviation, based on independent triplicates ( $n=3$ ).

Reactor	$q_{tot}/\text{C}$				$j_{max}/\mu\text{A cm}^{-2}$				$CE/\%$				$E^f/\text{V}$	
	1 <sup>st</sup>	2 <sup>nd</sup>	3 <sup>rd</sup>	4 <sup>th</sup>	1 <sup>st</sup>	2 <sup>nd</sup>	3 <sup>rd</sup>	4 <sup>th</sup>	1 <sup>st</sup>	2 <sup>nd</sup>	3 <sup>rd</sup>	4 <sup>th</sup>	After 1 <sup>st</sup> cycle	After 4 <sup>th</sup> cycle
BES	32.8 $\pm 0.6$	38.7 $\pm 3.8$	28.4 $\pm 4.0$	28.8 $\pm 4.8$	122.4 $\pm 22.9$	79.3 $\pm 17.3$	56.3 $\pm 6.5$	64.5 $\pm 12.7$	0.7 $\pm 0.0$	1.1 $\pm 0.1$	0.9 $\pm 0.1$	1.0 $\pm 0.1$	0.2 $\pm 0.0$	0.2 $\pm 0.1$
Split-BES after 4 <sup>th</sup> batch cycle	cells	46.1 $\pm 4.2$			84.6 $\pm 4.0$				2.6 $\pm 0.4$				0.0 $\pm 0.0$	
	WE	32.5 $\pm 8.1$			55.6 $\pm 9.2$				1.7 $\pm 0.5$				0.1 $\pm 0.0$	
Abiotic	11.2 $\pm 1.5$			10.6 $\pm 2.1$				-				-		
Autoclaved inoculum	13.8 $\pm 1.9$			7.7 $\pm 2.3$				-				-		

To shed further light on the EET, CV with a scan rate of  $1 \text{ mV s}^{-1}$  was performed at the maximum of the current production (turnover conditions) at the end of the 1<sup>st</sup> and the 4<sup>th</sup> batch cycle (Figure SI-1). In turnover conditions a formal potential of the EET ( $E^f$ ) of  $0.23 \pm 0.01 \text{ V}$  after the 1<sup>st</sup> cycle and  $0.16 \pm 0.07 \text{ V}$  after the 4<sup>th</sup> cycle (at  $\text{pH} = 4.8$  – Figure SI-1) was revealed. As abiotic controls did not yield a CV signal, this clearly demonstrates that microbial electrocatalysis takes place. Interestingly, the here identified  $E^f$  is close to  $E^f$  found for *C. cochlearium* of  $+0.22 \pm 0.05 \text{ V}$  [8].

To further identify the nature of the EET, an in-depth study was performed at the end of the 1<sup>st</sup> and the 4<sup>th</sup> cycle. Therefore, each original BES was split in three different components that were studied individually in fresh BES using CV as follows (details see 2.5): A) the WE (and the putative electroactive biofilm); B) the microorganisms, *i.e.* the cell pellet obtained by centrifugation of the used medium; C) the supernatant derived from centrifugation.

The CVs (Figure 2 and Figure SI-2) demonstrated that the planktonic cells ( $E^f = 0.04 \pm 0.01 \text{ V}$  at  $\text{pH} 8.1$ ,  $n=2$ ) being present in the used medium are responsible for the microbial electrochemical activity reported in the CA (Figure 1). In contrast, it was not possible to identify a  $E^f$  for the WE/biofilm and the supernatant.

The shift the  $E^f$  of the EET of around  $0.2 \text{ V}$  between the BES used for cultivation and the CVs obtained for the transferred cell pellet and WE can be explained by a pH-shift. The value is in line with a shift of  $60 \text{ mV/pH-unit}$  concomitant with the drop in pH in the WE chamber from  $8.1$  and  $4.8$  at the beginning and at the end of the batch cycle, respectively (see Figure SI-3). This change of pH during cultivation can be explained by the metabolic activity [33] leading to increasing concentration of short chain fatty acids by anaerobic fermentation of glucose. Pre-experiments

were conducted in similar conditions using only short chain fatty acids as carbon source, but here no bioelectrochemical signal (*i.e.* current production) was detected.

After the 4<sup>th</sup> batch cycle, in addition to the electrochemical activity of the planktonic cells ( $E^f=0.03\pm 0.02$  V at pH 8.1,  $n=3$ ) also the CVs of the WE/biofilm showed electrochemical activity ( $E^f=0.14\pm 0.00$  V at pH 8.1,  $n=3$ ). The activity of the latter could be due to the formation of an electroactive biofilm, but also the adherence of electroactive cells from the planktonic phase. Also in this case no  $E^f$  could be identified for the supernatant.

After the CV analysis, the WEs and the cells were further cultivated using CA for a full batch cycle, thereby showing electrochemical activity for 19h (Figure SI-3).

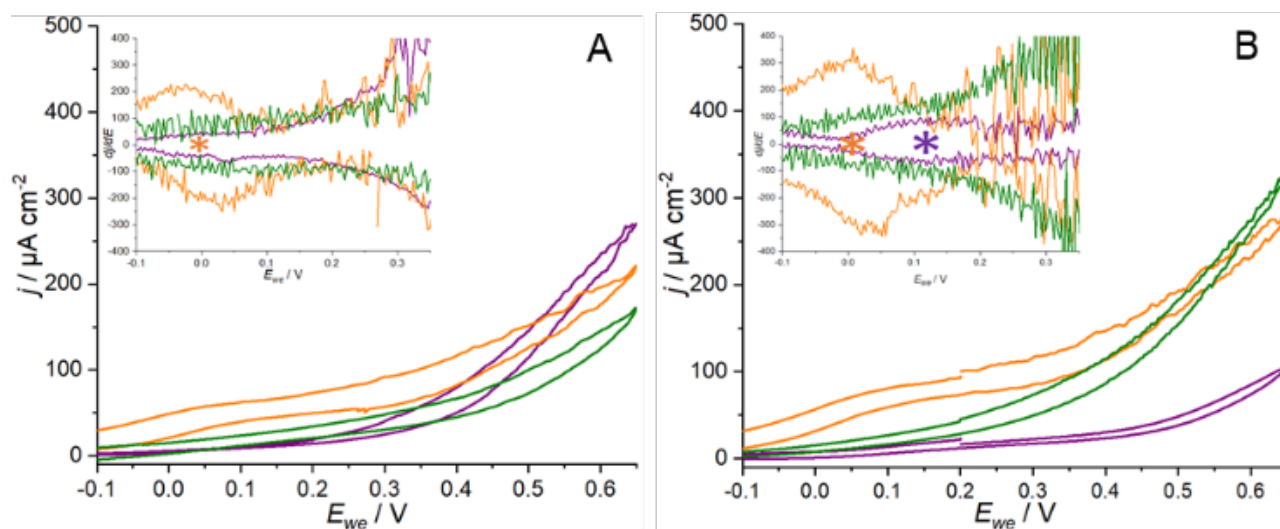


**Figure 2:** Representative CVs (scan rate of  $1 \text{ mV s}^{-1}$ ) and the respective 1<sup>st</sup> derivative (inset) using the cells (yellow), the WE/biofilm (purple) and the supernatant (green) of one of the triplicated bioelectrochemical system (BES1) at the end of the 1<sup>st</sup> (A) and of the 4<sup>th</sup> (B) batch cycles (see the data of the other replicates in Figure SI-2). The asterisk indicates the formal potential of the EET.

At the end of the experiment, the WEs were gently rinsed for removing the cells being not attached, cut into pieces and used for microbial analysis and microscopy. Figure 3 shows the presence of microbial cells at the surface of all WE, this may indicate that a biofilm being possibly electroactive is formed.

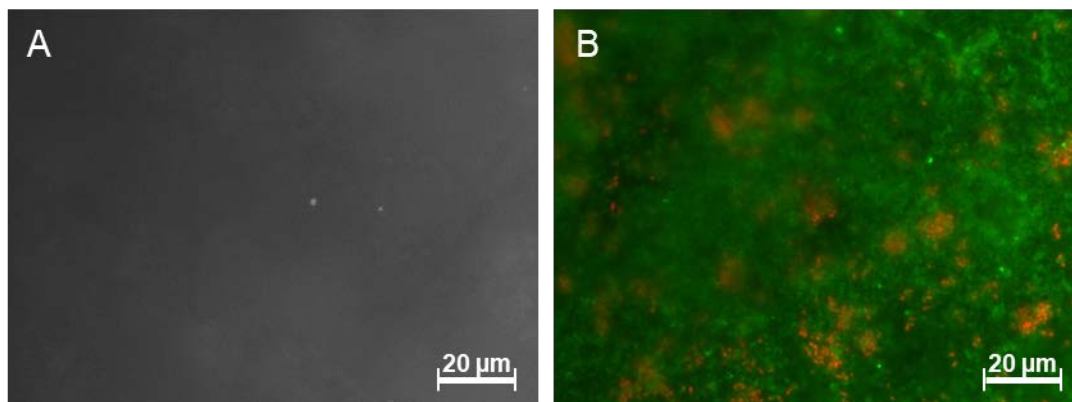


**Figure 3.** Comparison between the pictures obtained using optical microscope from: A) a new WE cleaned with sandpaper and B) the WEs of one of the triplicate bioelectrochemical systems (BES2), treated with the nucleic acid staining kit LIVE/DEAD® BacLight™ Bacterial Viability Kit (see Figure SI-4 for the rest of the data).

Subsequently, it was aimed to decipher the microbial community and identify the microbial electrocatalyst(s). Therefore, samples for DNA extraction were taken from the inoculum, the medium (at the end of each batch cycle) and from the WE (at the end of the experiment). The microbial community of the samples was analyzed using 16S rRNA gene amplicon sequencing (Illumina Miseq – Figure 4). All samples, except the inoculum, were characterized by a high dominance of the *Escherichia/Shigella* genus (98.05±0.03%, n=15).

Surprisingly this high selection of the *Escherichia/Shigella* genus was not only found for the BES but also for the open circuit controls (OC - 98.52%±0.02%, n=12 – Figure 4C).

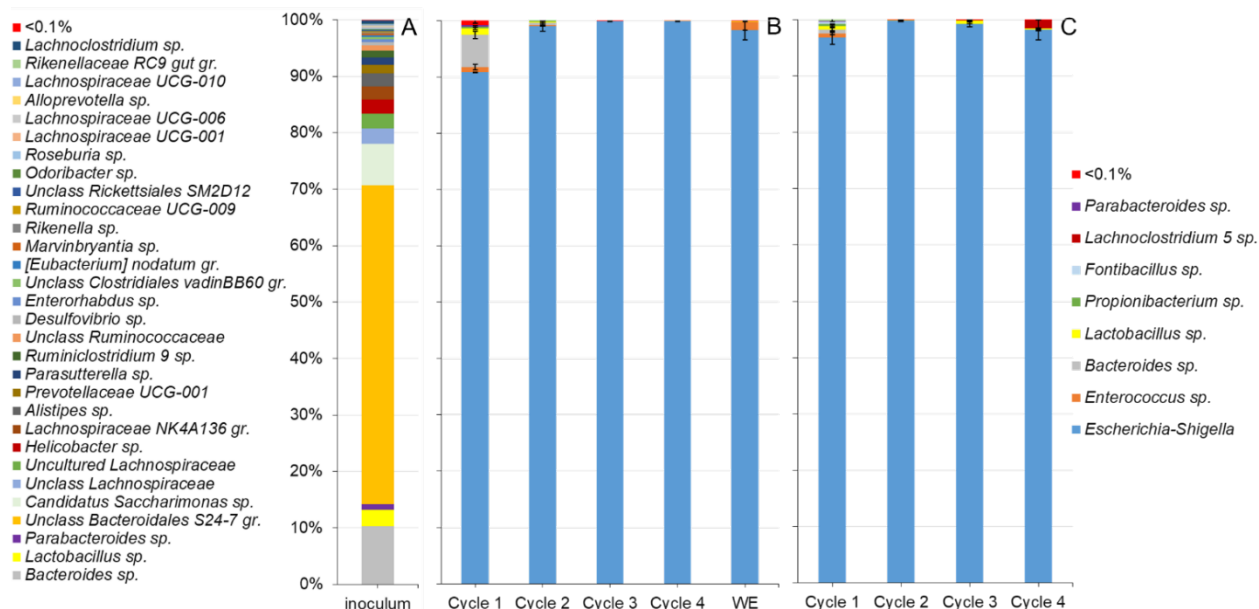


**Figure 4.** Genus distribution with the bacterial 16S rRNA gene amplicon sequencing (Illumina Miseq) of: A) the inoculum (mouse feces mixture: 100 pieces of C57BL/6NTac mouse feces in 20 mL of PBS 1x stored 24h at 4°C); B) the averaged data (n=3) of the pellet of the suspended cells at the end of each batch cycle and from the working electrodes at the end of the experiment and; C) the averaged data (n=3) of the pellet of the suspended cells at the end of each batch

cycle from the open circuit controls (OC). The detailed data are reported in the Supplementary Information 2.

Noteworthy, this analysis is involving a PCR-based amplification of the DNA that might lead to qualitative and quantitative amplification bias, mainly related to the use of specific primers [34]. To exclude a potential bias due to the use of primers, the PCR-free Nanopore sequencing was performed on three representative samples: the pelleted cells and the WE/biofilm of one BES and the pelleted cells of one OC. No visible biofilm was formed on the OC graphite rods.

This metagenomic analysis confirmed the 16S rRNA gene amplicon sequencing results (Figure 4). The strain with the highest abundance ( $86.5 \pm 13.3\%$  of completeness and  $0.6 \pm 0.1\%$  of contamination and a similarity of 99% between the samples - further details in Tables SI-1 to SI-3) was classified as *Escherichia flexneri* GCA\_002950215 via GTDB-TK and as *Shigella flexneri* 2a str. 301 with NCBI Strain Identifiers. The different classification is due to the fact that the *Shigella* genus is closely related to the *Escherichia* group [35].

The high presence of *Escherichia/Shigella* in all samples is certainly surprising and can hence not be related to pure electrochemically driven selection, as e.g. found for *Geobacter anodireducens* from waste water [36]. The selection has to be assigned to all experimental conditions (medium, anoxic condition, pH) and the use of glucose as substrate. It was previously demonstrated that the presence of sugar as carbon source in BES is contributing to the selection of the genus *Escherichia/Shigella* (up to  $20 \pm 9\%$  sucrose-fed BES and below 1% in the BES not fed with sucrose) [37] in anodic conditions.

In any case, these results strongly underline the importance of comprehensive controls when performing screenings for new electroactive microorganisms. Without these controls, a false-positive assignment can easily occur, as the increased abundance of a microorganism might be not due to electrochemically driven selection, but to the environmental pressure of the other experimental conditions.

On the other hand, the clinical isolate strain *S. flexneri* has been already reported for its capability to be electroactive in cathodic conditions [38]. Further, virulence of *S. flexneri* was associated, as other pathogenic electroactive microorganisms such as *Listeria Monocytogenes*, *Enterococcus faecalis* and *Pseudomonas aeruginosa* [5,39–41], to an iron based-binding protein (such as heme-binding protein) [42]. However, Pankratova et al. [9], have shown that *E. faecalis* and similar gram-positive bacteria, can perform EET without the use of heme-proteins (such as cytochromes), but need the aid of Osmium redox polymer (Os RP) or soluble monomeric redox mediators.

The obtained full genome sequence was annotated and the putative marker genes for electroactivity already used in a previous study [8], were analyzed.

**Table 3.** Abundance of putative marker genes in the strain sequenced in this study are compared to the model electroactive microorganisms *Geobacter sulfurreducens* and *Shewanella oneidensis* and the commensal gut microorganisms (*Clostridium cochlearium*, *Lactobacillus reuteri* and *Staphylococcus xylosus*) previously related to the EET mechanisms [8].

		<i>G. sulfurreducens</i>	<i>S. oneidensis</i>	<i>C. cochlearium</i>	<i>L. reuteri</i>	<i>S. xyloso</i>	<i>S. flexneri</i> (this study)
<b>Putative marker genes for electroactivity</b>	Cytochromes [31]	122	90	2	6	14	40
	Pilin [32]	1	9	-	-	-	8
	PilA [32]	2	1	-	-	-	-
	Ferredoxin [31]	33	11	21	-	4	20
	Nanotubes (YmdB) [32]	1	-	1	-	1	-
	Phosphodiesterase [32]	5	17	4	3	7	54

As Table 3 shows that the metagenome assembled genome (MAG) of the strain enriched in this study, is rich in genes putatively encoding components needed for electroactivity. This support the putative ability of *S. flexneri* to perform EET. In summary, we speculate that *S. flexneri* is a facultative electroactive microorganism in anodic conditions.

Recently, Keogh et al. [39] demonstrated that the presence of iron promoted the EET biofilm-specific metabolism capability of the *E. faecalis*, causing increased energy production and augmented biofilm growth. They reason that this potential metabolic versatility of *E. faecalis* and other gut pathogenic microorganisms supports their capability to colonize different niches and their survival in different complex niches (such as the human gastrointestinal tract). That allows us to speculate that *Shigella flexneri 2a str. 301* has a versatile electroactive metabolism.

*S. flexneri* is one of the main human pathogens causing diarrhea and shigellosis is associated with high morbidity and mortality in developing countries [43,44]. Recently, the commensal microbial community composition present in the host gut was demonstrated to be highly important for the establishment of a Shigella infection [43]. However, basic mechanisms of colonization and the interaction of Shigella with the other gut microorganisms need further research [43,44]. In this direction, the study of a different metabolic route associated with an EET mechanism could be a further important thread in this research line.

In this study (SI-4 and SI-5 files), several of the most important metabolic pathways for converting glucose into pyruvate as well as the full genetic metabolic routes for nitrate metabolism were found in all the samples (WE, BES1 and OC1). In contrast, the pathway for methanogenesis was not present. However, only metagenomic analysis is not sufficient to ascribe the metabolic activity and hence the fate of carbon to certain pathways, for which metatranscriptomic and/or metaproteomic analysis are required. Thus, in future pure culture studies under different conditions are required for further deciphering the potential facultative electroactive metabolism. We advocate that these include, for instance, the simultaneous metatranscriptomic and/or metaproteomic analysis of BES and open circuit controls, to evaluate the expression of the already discussed putative marker genes for electroactivity.

## 4. Conclusions

This study represents a new confirmation of the presence of electroactive microorganisms in the mammalian gut microbiome using electrochemical enrichment from mixed cultures. The samples (feces) from the common inbred strain of C57BL/6NTac mice were used to inoculate the triplicated bioelectrochemical reactors demonstrating the extracellular electron transfer and current production ( $j_{max}=122\pm 23 \mu\text{A cm}^{-2}$ ). The formation of biofilms at the anode being possibly electroactive was demonstrated using fluorescence microscopy and cyclic voltammetry ( $E^f=0.23\pm 0.01 \text{ V vs. Ag/AgCl sat. KCl}$ ). The 16S rRNA gene sequencing and PCR-free Nanopore sequencing showed the enrichment and dominance of *Shigella flexneri 2a str. 301*, with the identification of the genomic presence of several putative marker genes for electroactivity. The EET in gut microbiome opens interesting perspectives (e.g. prebiotics, drugs and an improved diet) aiming to host-microbiome interaction and health.

## Acknowledgements

We thank Dr. Claus Härtig, Katharina Neubert and Anne Kuchenbuch for the technical support with the gas chromatography and the optical microscopy. This work was supported by the Helmholtz Association within the Research Program Renewable Energies.

## References

- [1] Z.Y. Kho, S.K. Lal, The Human Gut Microbiome – A Potential Controller of Wellness and Disease, *Front. Microbiol.* 9 (2018) 1–23. doi:10.3389/fmicb.2018.01835.
- [2] J. Wang, T. Lang, J. Shen, J. Dai, L. Tian, X. Wang, Core gut bacteria analysis of healthy mice, *Front. Microbiol.* 10 (2019) 1–14. doi:10.3389/fmicb.2019.00887.
- [3] F. Hugenholtz, W.M. de Vos, Mouse models for human intestinal microbiota research: a critical evaluation, *Cell. Mol. Life Sci.* 75 (2018) 149–160. doi:10.1007/s00018-017-2693-8.
- [4] C. Koch, F. Harnisch, Is there a Specific Ecological Niche for Electroactive Microorganisms?, *ChemElectroChem.* 3 (2016) 1282–1295. doi:10.1002/celec.201600079.
- [5] S.H. Light, L. Su, R. Rivera-Lugo, J.A. Cornejo, A. Louie, A.T. Iavarone, C.M. Ajo-Franklin, D.A. Portnoy, A flavin-based extracellular electron transfer mechanism in diverse Gram-positive bacteria, *Nature.* 562 (2018) 140–144. doi:10.1038/s41586-018-0498-z.
- [6] S.H. Light, R. Méheust, J.L. Ferrell, J. Cho, D. Deng, M. Agostoni, A.T. Iavarone, J.F. Banfield, S.E.F. D'Orazio, D.A. Portnoy, Extracellular electron transfer powers flavinylated extracellular reductases in Gram-positive bacteria, *Proc. Natl. Acad. Sci.* 116 (2019) 26892–26899. doi:10.1073/pnas.1915678116.
- [7] I. Lagkouvardos, R. Pukall, B. Abt, B.U. Foessel, J.P. Meier-Kolthoff, N. Kumar, A. Bresciani, I. Martínez, S. Just, C. Ziegler, S. Brugiroux, D. Garzetti, M. Wenning, T.P.N. Bui, J. Wang, F. Hugenholtz, C.M. Plugge, D.A. Peterson, M.W. Hornef, J.F. Baines, H. Smidt, J. Walter, K. Kristiansen, H.B. Nielsen, D. Haller, J. Overmann, B. Stecher, T. Clavel, The Mouse Intestinal Bacterial Collection (miBC) provides host-specific insight into cultured diversity and functional potential of the gut microbiota, *Nat. Microbiol.* 1 (2016) 16131. doi:10.1038/nmicrobiol.2016.131.
- [8] L. Schwab, L. Rago, C. Koch, F. Harnisch, Identification of *Clostridium cochlearium* as an electroactive microorganism from the mouse gut microbiome, *Bioelectrochemistry.* 130 (2019) 107334. doi:10.1016/j.bioelechem.2019.107334.

- [9] G. Pankratova, D. Leech, L. Gorton, L. Hederstedt, Extracellular Electron Transfer by the Gram-Positive Bacterium *Enterococcus faecalis*, *Biochemistry*. 57 (2018) 4597–4603. doi:10.1021/acs.biochem.8b00600.
- [10] D. Naradasu, A. Guionet, T. Okinaga, T. Nishihara, A. Okamoto, Electrochemical Characterization of Current-Producing Human Oral Pathogens by Whole-Cell Electrochemistry, *ChemElectroChem*. (2020) 2012–2019. doi:10.1002/celec.202000117.
- [11] W. Wang, Y. Du, S. Yang, X. Du, M. Li, B. Lin, J. Zhou, L. Lin, Y. Song, J. Li, X. Zuo, C. Yang, Bacterial Extracellular Electron Transfer Occurs in Mammalian Gut, *Anal. Chem*. 91 (2019) 12138–12141. doi:10.1021/acs.analchem.9b03176.
- [12] D. Naradasu, W. Miran, M. Sakamoto, A. Okamoto, Isolation and Characterization of Human Gut Bacteria Capable of Extracellular Electron Transport by Electrochemical Techniques, *Front. Microbiol.* 9 (2019) 3267. doi:10.3389/fmicb.2018.03267.
- [13] A.C. Ericsson, D.J. Davis, C.L. Franklin, C.E. Hagan, Exoelectrogenic capacity of host microbiota predicts lymphocyte recruitment to the gut, *Physiol. Genomics*. 47 (2015) 243–252. doi:10.1152/physiolgenomics.00010.2015.
- [14] C. Koch, F. Harnisch, What is the essence of microbial electroactivity?, *Front. Microbiol.* 7 (2016) 1–5. doi:10.3389/fmicb.2016.01890.
- [15] X. Ze, S.H. Duncan, P. Louis, H.J. Flint, *Ruminococcus bromii* is a keystone species for the degradation of resistant starch in the human colon, (2012) 1535–1543. doi:10.1038/ismej.2012.4.
- [16] M.S. Desai, A.M. Seekatz, N.M. Koropatkin, N. Kamada, C.A. Hickey, M. Wolter, N.A. Pudlo, S. Kitamoto, A. Muller, V.B. Young, B. Henrissat, P. Wilmes, T.S. Stappenbeck, G. Núñez, E.C. Martens, A dietary fiber-deprived gut microbiota degrades the colonic mucus barrier and enhances pathogen susceptibility, 167 (2017) 1339–1353. doi:10.1016/j.cell.2016.10.043.A.
- [17] R. Hegner, C. Koch, V. Riechert, F. Harnisch, Microbiome-based carboxylic acids production: from serum bottles to bioreactors, *RSC Adv.* 7 (2017) 15362–15371. doi:10.1039/C6RA28259H.
- [18] A. Klindworth, E. Pruesse, T. Schweer, J. Peplies, C. Quast, M. Horn, F.O. Glöckner, Evaluation of general 16S ribosomal RNA gene PCR primers for classical and next-generation sequencing-based diversity studies, *Nucleic Acids Res.* 41 (2013) e1–e1. doi:10.1093/nar/gks808.
- [19] M. Martin, Cutadapt removes adapter sequences from high-throughput sequencing reads, *EMBnet.Journal.* 17 (2011) 10. doi:10.14806/ej.17.1.200.
- [20] B.J. Callahan, P.J. McMurdie, M.J. Rosen, A.W. Han, A.J.A. Johnson, S.P. Holmes, DADA2: High-resolution sample inference from Illumina amplicon data, *Nat. Methods*. 13 (2016) 581–583. doi:10.1038/nmeth.3869.
- [21] E. Bolyen, J.R. Rideout, M.R. Dillon, N.A. Bokulich, C.C. Abnet, G.A. Al-Ghalith, H. Alexander, E.J. Alm, M. Arumugam, F. Asnicar, Y. Bai, J.E. Bisanz, K. Bittinger, A. Brejnrod, C.J. Brislawn, C.T. Brown, B.J. Callahan, A.M. Caraballo-Rodríguez, J. Chase, E.K. Cope, R. Da Silva, C. Diener, P.C. Dorrestein, G.M. Douglas, D.M. Durall, C. Duvall, C.F. Edwards, M. Ernst, M. Estaki, J. Fouquier, J.M. Gauglitz, S.M. Gibbons, D.L. Gibson, A. Gonzalez, K. Gorlick, J. Guo, B. Hillmann, S. Holmes, H. Holste, C. Huttenhower, G.A. Huttley, S. Janssen, A.K. Jarmusch, L. Jiang, B.D. Kaehler, K. Bin Kang, C.R. Keefe, P. Keim, S.T. Kelley, D. Knights, I. Koester, T. Kosciulek, J. Kreps, M.G.I. Langille, J. Lee, R. Ley, Y.-X. Liu, E. Lofffield, C. Lozupone, M. Maher, C. Marotz, B.D. Martin, D. McDonald, L.J. McIver, A. V. Melnik, J.L. Metcalf, S.C. Morgan, J.T. Morton, A.T. Naimey, J.A. Navas-Molina, L.F. Nothias, S.B. Orchanian, T. Pearson, S.L. Peoples, D. Petras, M.L. Preuss, E. Pruesse, L.B. Rasmussen, A. Rivers, M.S. Robeson, P. Rosenthal, N. Segata, M. Shaffer, A. Shiffer, R. Sinha, S.J. Song, J.R. Spear, A.D. Swafford, L.R. Thompson, P.J. Torres, P. Trinh, A. Tripathi, P.J. Turnbaugh, S. Ul-Hasan, J.J.J. van der Hoof, F. Vargas, Y. Vázquez-Baeza, E. Vogtmann, M. von Hippel, W. Walters, Y. Wan, M. Wang, J. Warren, K.C. Weber, C.H.D. Williamson, A.D. Willis, Z.Z. Xu, J.R. Zaneveld, Y. Zhang, Q. Zhu, R. Knight, J.G. Caporaso, *Reproducible*,

- interactive, scalable and extensible microbiome data science using QIIME 2, *Nat. Biotechnol.* 37 (2019) 852–857. doi:10.1038/s41587-019-0209-9.
- [22] S.J. McIlroy, R.H. Kirkegaard, B. McIlroy, M. Nierychlo, J.M. Kristensen, S.M. Karst, M. Albertsen, P.H. Nielsen, MiDAS 2.0: an ecosystem-specific taxonomy and online database for the organisms of wastewater treatment systems expanded for anaerobic digester groups, *Database.* 2017 (2017). doi:10.1093/database/bax016.
- [23] P. Menzel, K.L. Ng, A. Krogh, Fast and sensitive taxonomic classification for metagenomics with Kaiju, *Nat. Commun.* 7 (2016) 11257. doi:10.1038/ncomms11257.
- [24] S. Koren, B.P. Walenz, K. Berlin, J.R. Miller, N.H. Bergman, A.M. Phillippy, Canu: scalable and accurate long-read assembly via adaptive k -mer weighting and repeat separation, *Genome Res.* 27 (2017) 722–736. doi:10.1101/gr.215087.116.
- [25] J. Alneberg, B.S. Bjarnason, I. de Bruijn, M. Schirmer, J. Quick, U.Z. Ijaz, L. Lahti, N.J. Loman, A.F. Andersson, C. Quince, Binning metagenomic contigs by coverage and composition, *Nat. Methods.* 11 (2014) 1144–1146. doi:10.1038/nmeth.3103.
- [26] L.M. Rodriguez-R, S. Gunturu, W.T. Harvey, R. Rosselló-Mora, J.M. Tiedje, J.R. Cole, K.T. Konstantinidis, The Microbial Genomes Atlas (MiGA) webserver: taxonomic and gene diversity analysis of Archaea and Bacteria at the whole genome level, *Nucleic Acids Res.* 46 (2018) W282–W288. doi:10.1093/nar/gky467.
- [27] P.-A. Chaumeil, A.J. Mussig, P. Hugenholtz, D.H. Parks, GTDB-Tk: a toolkit to classify genomes with the Genome Taxonomy Database, *Bioinformatics.* (2019). doi:10.1093/bioinformatics/btz848.
- [28] D.H. Parks, M. Imelfort, C.T. Skennerton, P. Hugenholtz, G.W. Tyson, CheckM: assessing the quality of microbial genomes recovered from isolates, single cells, and metagenomes, *Genome Res.* 25 (2015) 1043–1055. doi:10.1101/gr.186072.114.
- [29] M.R. Olm, C.T. Brown, B. Brooks, J.F. Banfield, DRep: A tool for fast and accurate genomic comparisons that enables improved genome recovery from metagenomes through de-replication, *ISME J.* 11 (2017) 2864–2868. doi:10.1038/ismej.2017.126.
- [30] T. Brettin, J.J. Davis, T. Disz, R.A. Edwards, S. Gerdes, G.J. Olsen, R. Olson, R. Overbeek, B. Parrello, G.D. Pusch, M. Shukla, J.A. Thomason, R. Stevens, V. Vonstein, A.R. Wattam, F. Xia, RASTtk: A modular and extensible implementation of the RAST algorithm for building custom annotation pipelines and annotating batches of genomes, *Sci. Rep.* 5 (2015) 8365. doi:10.1038/srep08365.
- [31] D.R. Lovley, *Electromicrobiology*, *Annu. Rev. Microbiol.* 66 (2012) 391–409. doi:10.1146/annurev-micro-092611-150104.
- [32] D.R. Lovley, Happy together: microbial communities that hook up to swap electrons, *ISME J.* 11 (2017) 327–336. doi:10.1038/ismej.2016.136.
- [33] R.A. Rozendal, H.V.M. Hamelers, C.J.N. Buisman, Effects of Membrane Cation Transport on pH and Microbial Fuel Cell Performance †, *Environ. Sci. Technol.* 40 (2006) 5206–5211. doi:10.1021/es060387r.
- [34] H. Krehenwinkel, M. Wo, J.Y. Lim, A.J. Rominger, W.B. Simison, R.G. Gillespie, Estimating and mitigating amplification bias in qualitative and quantitative arthropod metabarcoding, (2017) 1–12. doi:10.1038/s41598-017-17333-x.
- [35] Q. Jin, Z. Youan, J. Xu, Y. Wang, Y. Shen, W. Lu, J. Wang, H. Liu, J. Yang, F. Yang, X. Zhang, J. Zhang, G. Yang, H. Wu, Q. Di, D. Jie, L. Sun, Y. Xue, A. Zhao, Y. Gao, J. Zhu, B. Kan, K. Jung Yu, Genome sequence of *Shigella flexneri* 2a: insights into pathogenicity through comparison with genomes of *Escherichia coli* K12 and O157, *Nucleic Acids Res.* 30 (2002) 4432–4441. doi:10.1093/nar/gkf566.
- [36] F. Harnisch, C. Koch, S. a. Patil, T. Hübschmann, S. Müller, U. Schröder, Revealing the electrochemically driven selection in natural community derived microbial biofilms using flow-cytometry, *Energy Environ. Sci.* 4 (2011) 1265. doi:10.1039/c0ee00605j.
- [37] C. Koch, K.J. Huber, B. Bunk, J. Overmann, F. Harnisch, Trophic networks improve the performance of microbial anodes treating wastewater, *Npj Biofilms Microbiomes.* 5 (2019) 1–9. doi:10.1038/s41522-019-0100-y.
- [38] A. Cournet, M. Délia, A. Bergel, C. Roques, M. Bergé, Electrochemical reduction of

- oxygen catalyzed by a wide range of bacteria including Gram-positive, *Electrochem. Commun.* 12 (2010) 505–508. doi:10.1016/j.elecom.2010.01.026.
- [39] D. Keogh, L.N. Lam, L.E. Doyle, A. Matysik, S. Pavagadhi, S. Umashankar, P.M. Low, J.L. Dale, Y. Song, S.P. Ng, C.B. Boothroyd, G.M. Dunny, S. Swarup, R.B.H. Williams, E. Marsili, K.A. Kline, Extracellular Electron Transfer Powers *Enterococcus faecalis* Biofilm Metabolism, *MBio.* 9 (2018) 1–17. doi:10.1128/mBio.00626-17.
- [40] A. Reinhart, A. Oglesby-Sherrouse, Regulation of *Pseudomonas aeruginosa* Virulence by Distinct Iron Sources, *Genes (Basel).* 7 (2016) 126. doi:10.3390/genes7120126.
- [41] A. Cournet, M. Bergé, C. Roques, A. Bergel, M.-L. Délia, Electrochemical reduction of oxygen catalyzed by *Pseudomonas aeruginosa*, *Electrochim. Acta.* 55 (2010) 4902–4908. doi:10.1016/j.electacta.2010.03.085.
- [42] C.E. Stugard, P.A. Daskaleros, S.M. Payne, A 101-kilodalton heme-binding protein associated with Congo red binding and virulence of *Shigella flexneri* and enteroinvasive *Escherichia coli* strains, *Infect. Immun.* 57 (1989) 3534–3539.
- [43] M. Anderson, P.J. Sansonetti, B.S. Marteyn, *Shigella* Diversity and Changing Landscape: Insights for the Twenty-First Century, *Front. Cell. Infect. Microbiol.* 6 (2016). doi:10.3389/fcimb.2016.00045.
- [44] J. Yang, W. Chen, P. Xia, W. Zhang, Dynamic comparison of gut microbiota of mice infected with *Shigella flexneri* via two different infective routes, *Exp. Ther. Med.* (2020). doi:10.3892/etm.2020.8469.